journal

J. Am. Ceram. Soc., 92 [6] 1328–1332 (2009)
DOI: 10.1111/j.1551-2916.2009.03052.x

Formation of Oxide Films on ZrB_2–15 vol% SiC Composites During Oxidation: Evolution with Time and Temperature

Sigrun N. Karlsdottir† and John W. Halloran

Department of Materials Science and Engineering, University of Michigan, Ann Arbor, Michigan 48104

The evolution of convection cells features that form in oxide films on ZrB_2–SiC composites are quantified by the number population, size, and distribution in oxide films on ZrB_2–15 vol% SiC oxidized at temperatures between 1500° and 1600°C for various oxidation times. The number of convection cells per unit area increases after short exposure times of the oxidation at 1550°C, but then decreases slowly with increasing time. The results indicate that these convection cells are transient, they form and transport boria–silica–zirconia liquid to the surface but with increasing exposure time the increasing amount of flowing viscous SiO_2-rich liquid submerges them and they become extinct.

I. Introduction

During high-temperature oxidation of ZrB_2–SiC composites, it is well known that a borosilicate oxide (B_2O_3–SiO_2) film forms on the outer surface. Due to the high vapor pressure of boria ($B_2O_3(l)$) at these temperatures, compared with silica ($SiO_2(l)$), the B_2O_3 is preferentially evaporated from the borosilicate liquid. The liquid oxide film at the outer surface then becomes predominantly viscous SiO_2-rich borosilicate liquid.[1–4] Previously we proposed a novel oxidation mechanism where the flow of boria–silica–zirconia (BSZ) liquid plays an important role in the formation of oxide scales on these materials.[5–7] This mechanism was proposed to interpret distinctive microstructural features observed on the oxide films, which had the appearance of "islands" of ZrO_2 particles clustered on the outer surface of the oxide film. The zirconia islands were surrounded by a region of silica-rich glass, which resembled a "lagoon" surrounding the zirconia islands. Within the silica-rich lagoons, and adjacent to the zirconia islands were lobes of B_2O_3-rich glass arranged like the petals of a flower.[5] We interpreted these features as convection cells arising from flow of a liquid oxide solution containing boron oxide, silicon oxide, and zirconium oxide (BSZ liquid).[5–7]

Previously we proposed that the convection cells are formed by the flow of BSZ liquids to the surface, where subsequent evaporation of B_2O_3-rich liquid causes precipitation of crystalline zirconia (the ZrO_2 islands) and leaves a silica-rich remnant liquid (the SiO_2 lagoons).[6] The driving force for flow was proposed to be the very large volume increase upon oxidation of the bulk material due to the formation of condensed oxides, solid "primary" $ZrO_2(s)$ and BSZ liquid. The BSZ liquid forms underneath the oxide scale, at the reaction interface, where inward diffusing oxygen reacts with the SiC and ZrB_2 to form a porous layer of the primary zirconia and the BSZ liquid solution.[5,6] In the early stages, we presume that the BSZ liquid can flow through the pores of the primary zirconia layer in the thin oxide scale. At later stages, however, the very large volume increase caused by the formation of the BSZ liquid induces pressure and stresses leading to a rupture in the oxide scale. The BSZ liquid at the reaction interface is then squeezed up to the surface and starts flowing, forming the convection cells and their features.[7]

This paper is a more detailed analysis of the evolution of convection cells in oxide films on ZrB_2–15 vol% SiC composites involving the spatial distribution, morphology, and population of the convection cells as effected by the oxidation time mostly at 1550°C. We also report enhanced oxidation beneath the convection cell features.

II. Experimental Procedure

ZrB_2–15 vol% SiC composite provided by CNR-ISTEC (The Institute of Science and Technology for Ceramics, National Research Council) in Faenza, Italy. Properties and processing methods of the ZrB_2–15 vol% SiC composites are presented in more detail elsewhere.[8] Oxidation was conducted in a high-temperature box furnace (SentroTech Corporation, Berea, OH) in ambient air at 1550°C for 0.5, 1, 2, 3, 4, 6, and 8 h. The heating and cooling rates were 13°C/min.

The specimens were supported on pieces of the same material, which were placed on an Al_2O_3 support in an Al_2O_3 crucible. Before oxidation ca. 200 μm was removed from the surface with a fine diamond grid (Omni Brade, TBW Industries, Furlong, PA). This diamond grinding was carried out to remove any heat affected zone that could have formed during wire electrical discharge machining (Ann Arbor Machine Model 1S15, Ann Arbor, MI), that was used to cut the ZrB_2–SiC bulk material into thin sheets. The thin sheets of the ZrB_2–SiC were then cut with a diamond saw (IsoMet® 1000 diamond precision saw, Buehler, Lake Bluff, IL) into small rectangular coupons with total surface area on average of ca. 1 cm^2.

Microstructural analysis were carried out on the surfaces and cross-sections using scanning electron microscopy (SEM) and backscattering electron (BSE) microscopy. The cross-sections of the oxidized specimens were prepared for microstructural analysis by nonaqueous polishing procedures down to 1 μm finish. Specimens were coated with carbon before microstructure analysis. An X-ray Diffractometer (XRD) (Rigaku Miniflex, Rigaku Americas Corporation, TX) was used for XRD analysis of the surface of the specimens to identify the phases and structure of the oxides formed during oxidation.

III. Results: Analysis of Oxide Scales

(1) Microstructure Features on the Oxide Scale Surface

(A) Distribution and Population of Convection Cells: Figures 1(a)–(d) show BSE micrographs of surfaces of ZrB_2–15 vol% SiC (ZS) composites oxidized at 1550°C for 0.5, 1, 4, and 8 h. Herein the specimens will be referred to as ZS-05, ZS-1, etc.) The oxidized specimens have convection cells spread over the surfaces. The images in Fig. 1 are taken at low magnifications (× 36–38, 20 kV, spot size: 5) to be able to compare the

M. Cinibulk—contributing editor

Manuscript No. 24489. Received March 31, 2008; approved February 28, 2009.
This work was supported by the Office of Naval Research under contract N00014-02-1-0034.
†Author to whom correspondence should be addressed. e-mail: sigrunkarls@nmi.is

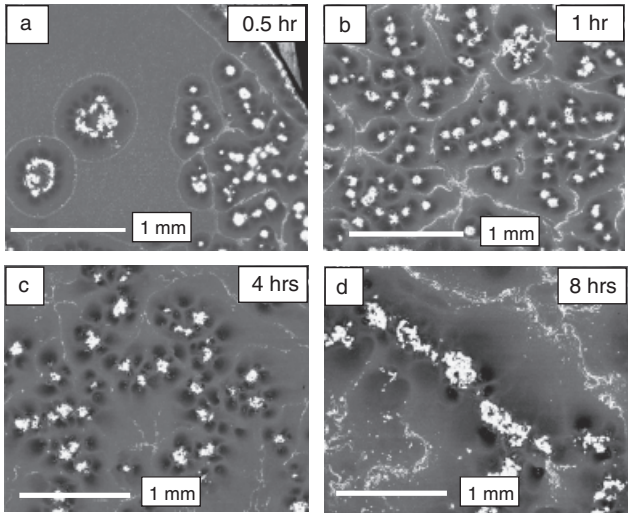

Fig. 1. Backscattering Electron images of surfaces of the ZrB_2–15 vol% SiC (ZS) composites tested at 1550°C from (a) 0.5 h ZS-05, (b) 1 h ZS-1, and (c) 4 h ZS-4, and (d) 8 h ZS-8.

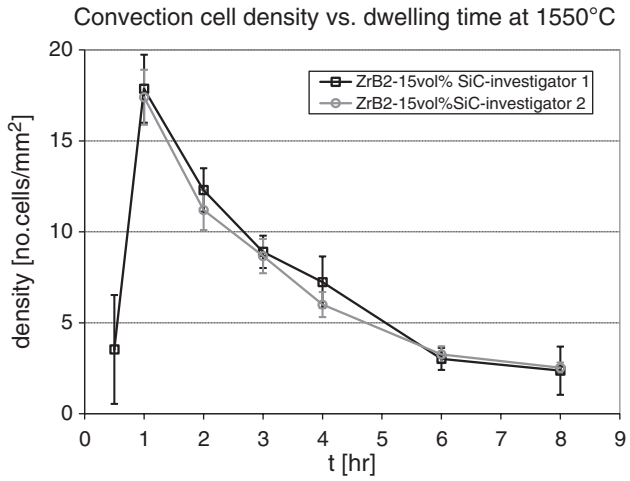

Fig. 2. The calculated density of the convection cells versus different oxidation times for the ZrB_2–SiC composite oxidized at 1550°C.

population of the convection cells between different oxidation times. The formation of convection cells and the chemical composition of their features (the B_2O_3 petals, the SiO_2 lagoons, and the ZrO_2 islands) have been explained in detail elsewhere.[5–7]

After 0.5 h of oxidation, specimen ZS-05, there are relatively few cells on the surface and the spatial distribution of the cells is not uniform. The field of view in Fig. 1(a) ZS-05 shows two isolated cells to the left and it has more closely packed cells on the right side of the specimen compared with left. After 1 h of oxidation there is a larger number of convection cells and they are more uniformly spread over the surface, as shown by the field of view for specimen ZS-1 in Fig. 1(b). The morphology and number of cells on these two specimens indicate that the population of the cells increases at 1550°C for oxidation time between 0.5 and 1 h. Also, the distribution of the cells for the ZS-05 specimen indicates that the cells form first rather sparsely on the surfaces but start to impinge when the population increases forming convection cell patterns similar to the one seen on the ZS-1 specimen. After 4 h, there seem to be a lower population of cells (Fig. 1(c), and still fewer after 8 h Fig. 1(d)), with the individual cells impinging on their neighbors.

Micrographs such as Figs. 1(b)–(d) show only limited fields of view. Multiple fields of view were examined to more systematically quantify the convection cells for each specimen. The number of convection cells per square millimeter (cell density: no./mm^2) were quantified by counting the numbers of cells on the samples in 15 random fields (a square frame; 1 mm × 1 mm) per sample at × 36–38 microscopic magnification. Because it is sometimes difficult to distinguish one cell from another, two separate investigators visually counted the cells in the samples in a blinded fashion. The cell counts were then averaged for each sample. This kind of quantification by visual counting is commonly used for manual quantification of features using microscopic imaging, e.g., in cell staining.[9,10]

Figure 2 shows the average number of convection cell features per square millimeter as a function of oxidation time. The number of cells/mm^2 varies with position on each sample, so we present an average from 15 randomly chosen areas, with the 95% confidence interval calculated for a Gaussian distribution. The graph shows that the data from both counts (investigator 1 and 2) are the same. After a population peak at ~1 h oxidation time, the number of cells/mm^2 decrease with time. The micrographs shown in Fig. 1 also indicate that the spatial distribution of the convection cells changes with oxidation time. The cells are more uniformly distributed over the surface for ZS-1, but tend to be more locally clustered to together for ZS-8. Interestingly, the surface of the ZS-8 specimen was not smooth, it had a hilly appearance, were there were large areas dominated by SiO_2 with hilly appearance and other regions dominated by clusters of convection cells. The population data in Fig. 2 are for randomly chosen locations.

(B) Size of Convection Cell Features: Further quantitative analyses were performed for the convection cells formed on the ZrB_2–SiC specimens tested at 1550°C from 1 to 8 h. One of the more distinctive features are the lobes of BSZ liquid, which create a "flower petal" pattern of B_2O_3-rich regions around each ZrO_2 island. To quantify the number of petals the average number of petals per island were determined for each specimen. The averages were calculated by dividing the total number of petals by the total number of ZrO_2 islands counted per field for each specimen. Fifteen random fields (1 mm × 1 mm frame) were used per sample on micrographs with an × 36–38 magnification. The number of petals per flower does not significantly change with increasing oxidation times, i.e. the average number of petals per flower for each oxidation time varies relatively little, from a minimum of 2.64 ± 0.49 (ZS-1) to a maximum 3.12 ± 0.79 (ZS-4). The overall average of the number of petals per flower is 2.83 ± 0.73. The relatively high error (1 standard deviation) could result from the dependence of the flower petals to the location, which then affects the calculated average number of petals per flower for each specimen.

The number of the petals per flower for the shortest oxidation time, 0.5 h (shown in Fig. 1(a)), is not as straightforward to interpret. For the newly formed convection cells shown in Fig. 1(a) it is not quite clear if the larger isolated cells to left on the micrograph are many small cells located together in a circle or if that is one isolated cell. We presume these are in fact smaller ones located near to each other, which then with time resemble the ones in the right corner of the micrograph. If that is true then the average number of petals per flower for 0.5 h is similar to the specimens oxidized at longer oxidation times, ca. three flower petals per cell.

The size of the B_2O_3 petals, the SiO_2 lagoons and the ZrO_2 islands were measured, and the average and standard error (± 1 standard deviation) was calculated for the different oxidation times. The sizes of the features were measured for each specimen during microstructure analysis using SEM. The diameter of the B_2O_3 petals, the SiO_2 lagoons, and the ZrO_2 islands were measured in x- and y-direction randomly. The values in x- and y-direction were very similar thus the measured size is the estimated diameter of the features. At least 20 values were used to calculate the average size for each exposure time. Figure 3 shows the results of these measurements; average sizes of the ZrO_2 islands, B_2O_3 petals, and SiO_2 lagoons formed on the ZrB_2–SiC composite tested at 1550°C, versus the various oxidation times.

The sizes of the ZrO_2 islands seem overall to increase with longer oxidation time. There seems to be three different trends

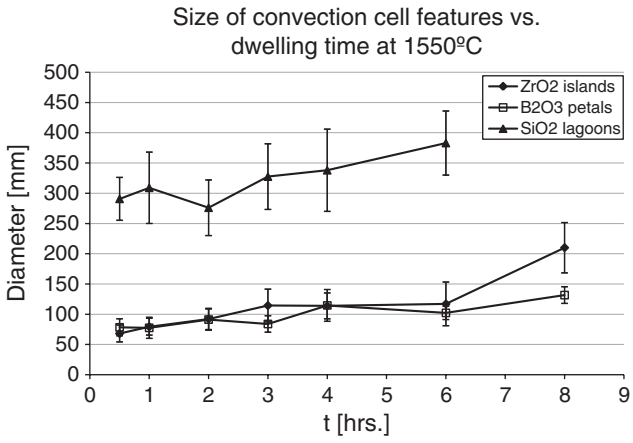

Fig. 3. The average size of ZrO_2 islands, B_2O_3 petals, and SiO_2 cells on the ZrB_2–SiC composites tested at 1550°C from 0.5 to 8 h.

in the data; an evident increase from 0.5 to 3 h.; no significant increase between 3 and 6 h; and then from 6 to 8 h there is a rapid increase in the size. During microstructure analysis of the ZS-8 specimen it became somewhat hard to distinguish one ZrO_2 island from another and some of them seem to have coalesced. Thus care was taken during measurements of the ZrO_2 islands for the ZS-8 specimen, to make sure that the measured diameter was of one island but not two. The increase in the size of the ZrO_2 could indicate that for the longer oxidation times, especially for 8 h, the ZrO_2 islands have possibly grown in the SiO_2-rich borosilicate melt and then started to coalesce together.

The size of the B_2O_3 petals, measured for each oxidation time at 1550°C, is also shown in Fig. 3. The size of the B_2O_3 petals seem to increase overall with longer oxidation time just as the ZrO_2 islands, the increase is smaller though and there is more variation in this pattern than for the sizes of ZrO_2. This could perhaps be interpreted as evidence for correlation between the size of the B_2O_3 petals and the ZrO_2 islands, which would support the authors' hypothesis about the composition dependence between B_2O_3 and ZrO_2 through the BSZ liquid formation. The size of the SiO_2 lagoons were measured and calculated for oxidation times from 0.5 to 6 h, this is also shown in Fig. 3. The size of the SiO_2 lagoons could not be measured for the 8 h oxidation time due to change in the shape of the lagoons with oxidation time, i.e. the SiO_2 lagoons on the ZS-05 specimen had well defined boundaries while the ZS-8 had no definite boundaries. This made measuring the sizes difficult. Thus the averages calculated from the measurements of the sizes of the SiO_2 lagoons should be taken with caution. Overall the sizes of the SiO_2 lagoons seem to increase with longer oxidation time just as the ZrO_2 islands and the B_2O_3 petals indicating that all these features are dependant.

(C) Dendrites of Zirconia Adjacent to the Zirconia Islands: Higher magnification of the ZrO_2 islands on the ZS-8 specimen shows large dendrites in the outer boundaries

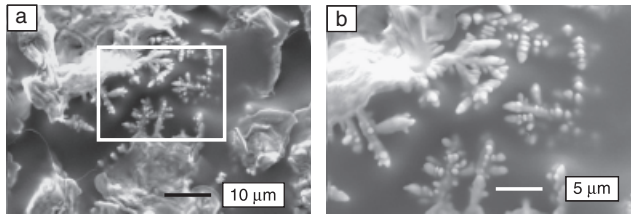

Fig. 4. Scanning electron micrographs of the dendrite features observed connected to one of the ZrO_2 islands on the surface of a ZrB_2–15 vol% SiC composite oxidized at 1550°C for 8 h (ZS-8). Figure 4(b) is a higher magnification of the area inside the white box in the micrograph in Fig. 4(a).

of the ZrO_2 islands, close to B_2O_3 petals, this is shown in Fig. 4. Interestingly, similar dendrites but somewhat smaller are seen close to the B_2O_3 petals on the edges of the ZrO_2 islands on the specimens oxidized for shorter times. Perhaps the ZrO_2 precipitates form as dendrites when there is super-saturation of zirconia in the BSZ liquid when the B_2O_3 starts evaporating away from liquid. The dendrites could then coalescence together and form the grains that are the main constitutes of the ZrO_2 islands. Epassaka *et al.*[11] found that for ZrO_2 crystallites, deposited by a chemical vapor deposition under atmospheric pressure on a silicon substrate underwent a morphological instability and formed a dendritic structure. They claimed that at higher substrate temperature, intermediate super-saturation favors the formation of the dendrites. Dendritic growth phenomena have also been seen for Cu–Hf–Ti–Ag–Ta bulk metallic glass composites where Ta rich-dendrites form by precipitation during fabrication of the composite.[12] For the precipitation of dendrites in under-cooled glass melts; at the beginning of spontaneous crystallization of an under-cooled melt, the growth occurs in preferred direction. Because conventional glass melts are very viscous the transport of new growth material by diffusion is slow and dendrites form.[13] Composition gradients and associated diffusion near crystal-melt interface are also known to affect crystal growth by causing the crystal to break up into a cellular morphology such as dendrites.[14] For our case, when the B_2O_3 starts evaporating away from the BSZ liquid the viscosity of the liquid will increase due to the increase in the SiO_2 amount for the overall composition of the liquid. Perhaps this induces the dendritic form of the precipitated ZrO_2. Also, from the crystal growth theory it is known that in melts that are controlled by diffusion or heat-flow cellular morphologies such as dendrites form during crystal growth.

Surface images of three ZrB_2–15% SiC specimens each oxidized for 0.5 h at different temperature; 1500°, 1550°, and 1600°C are shown in Fig. 5. Convection cells were observed on all three specimens. By comparing the images it can be seen that, for this temperature range, the number of convection cells increase with increasing temperature. The images also suggest that when more convection cells form, they form until they cover the surface and then start to impinge together. The increased number of convection cells for higher temperatures is likely due

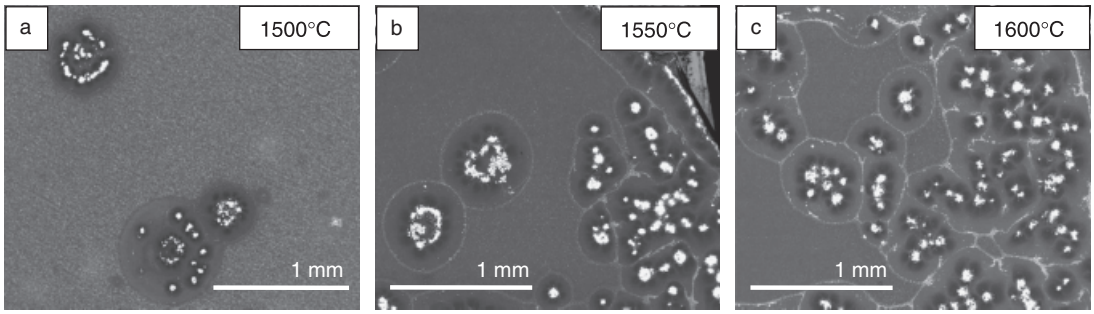

Fig. 5. Backscattering Electron images of the surface of ZrB_2–15 vol% SiC composite tested for a fixed time, 0.5 h, at different temperatures; (a) 1500°C, (b) 1550°C, and (c) 1600°C, respectively.

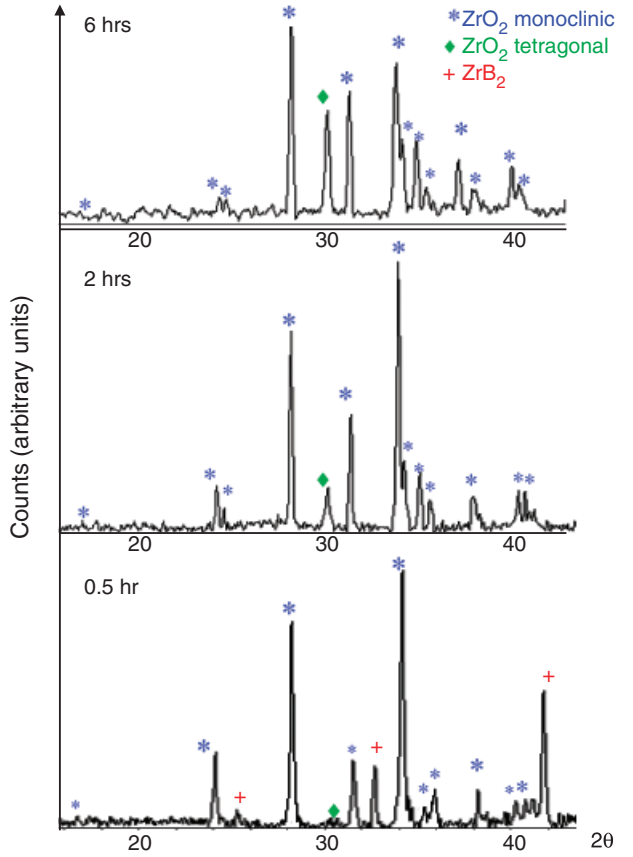

Fig. 6. X-ray diffraction patterns of the surface of ZrB_2–15 vol% SiC specimens oxidized at 1550°C for 0.5 h (bottom), 2 h, and 6 h (top). The phases identified are shown with different markers; ZrB_2 with open diamond, monoclinic α-ZrO_2 with snowflake, and tetragonal β-ZrO_2 with closed diamond.

to an increased evaporation rate of the B_2O_3 at increasing temperatures. When the B_2O_3 starts evaporating faster, the ZrO_2 precipitates form faster, which results in faster formation of the convection cells.

(2) XRD Surface analysis: Phase Composition and Structure

XRD analyses of the surface of the specimens were performed to get information about the phases and structure of the oxides. These results can be seen in Fig. 6. We looked for zircon ($ZrSiO_4$) that might form as a stable compound in the ternary system ZrO_2–B_2O_3–SiO_2. Zircon was predicted in a calculated ternary 1500°C isothermal section of the ZrO_2–B_2O_3–SiO_2 system.[6] No $ZrSiO_4$ was observed. This is not surprising because $ZrSiO_4$ has not been reported previously in the literature for similar ZrB_2–SiC composites oxidized at high temperatures (>1500°C). Both monoclinic and tetragonal zirconia was identified with monoclinic zirconia more abundant. There was more tetragonal zirconia for longer oxidation times. We presume that tetragonal zirconia formed during oxidation but transformed to monoclinic zirconia during cooling.

(3) Cross-sectional Analysis of Oxide Films

Figure 7 shows micrographs of cross-sections of the ZS specimens oxidized at 1550°C for 1 h (ZS-1), 4 h (ZS-4), and 8 h (ZS-8). The micrographs show enhanced oxidation zones (thicker oxide layer) under the ZrO_2 islands. The thickness of the SiO_2-rich surface layer and the ZrO_2 layer for each specimen tested was measured. The thickness for each layer was measured by averaging 20–30 values at various locations. Difficulties existed in measuring the average thickness due to the non-uniformity of the oxide layer, i.e. the enhanced oxidation zone under the convection cells. The enhanced oxidation zones under the ZrO_2 islands are discussed in detail elsewhere.[7] But in summary,

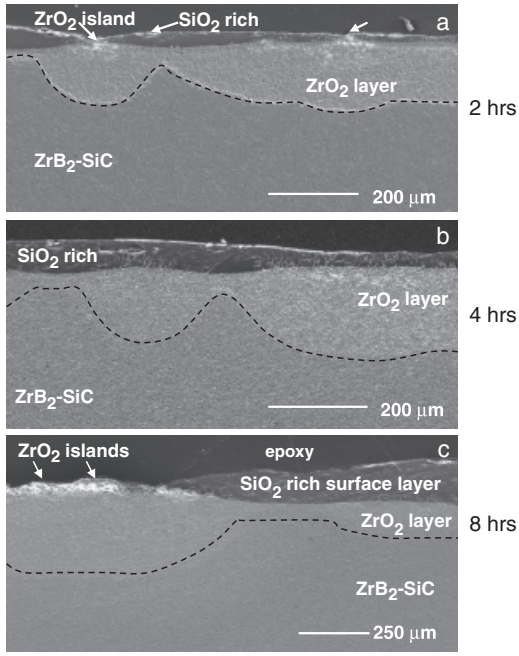

Fig. 7. Secondary electron micrographs of the cross-sections of ZrB_2–15 vol% SiC composites tested at 1550°C for (a) 2 h, (b) 4 h, and (c) 8 h, showing the large difference in the thickness of the oxide where the convection cells are located (ZrO_2 islands) compared with the area covered with SiO_2-rich surface layer. The interface between the ZrO_2 layer and the un-reacted bulk material is indicated with a broken line.

it forms when the BSZ liquid squeezes up to the surface, due to the large volume increase upon oxidation, which opens a path for more rapid inward oxygen diffusion due to the lower viscosity of the BSZ liquid compared with the surrounding SiO_2-rich surface layer.[7] (Note that the boria-rich petals seen in backscattered electrons on the oxide surface are not visible under the contrast conditions for Fig. 7 for scale cross-sections.) The nonuniformity is easily seen from Fig. 7. This resulted in large standard deviation of the thicknesses. The overall thickness of the oxide layer increases with increasing oxidation time as shown in Fig. 8, which shows the total thickness of the oxide layer (SiO_2-rich surface layer+underlying ZrO_2 layer) versus oxidation time (0.5 to 8 h) at 1550°C. The error is the standard deviation, $\pm\sigma$ where

$$\sigma = \sqrt{\sigma^2_{SiO_2 layer} + \sigma^2_{ZrO_2 layer}}$$

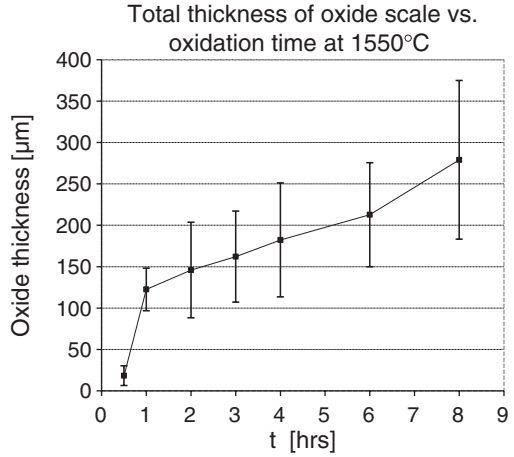

Fig. 8. The total oxide thickness of the ZrB_2–15 vol% SiC composites oxidized at various oxidation times from 0.5 to 8 h.

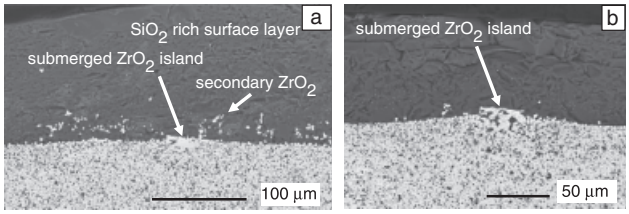

Fig. 9. Backscattering electron images of cross-sections of ZrB_2–15 vol% SiC specimens tested at 1550°C for (a) 8 h (ZS-8) and (b) 6 h (ZS-6) showing the SiO_2-rich surface layer (dark gray) and the underlying ZrO_2 (white contrast).

The total oxide thickness increases rapidly at the first stage of oxidation (between 0.5 and 1 h) but then steadily increases with time.

For the ZS specimens oxidized at 1550°C for 6 and 8 h microstructural analysis of the cross-sections revealed submerged ZrO_2 islands, completely covered with SiO_2 rich surface layer, this is shown in Figs. 9(a) and (b). This suggests that there were convection cells formed at earlier stage in the oxidation, but were later covered by the viscous SiO_2 liquid, presumably from the formation other adjacent convection cells or another source of flowing liquid oxide. We suggest that a zirconia island covered with silica represents a convection cell that has ceased to operate (as no fresh zirconia deposits). Recall that we believe that the zirconia in the islands precipitates from the BSZ liquid when the B_2O_3 evaporates at the surface. No evaporation occurs at a submerged island, because it is no longer at an external surface. The BSZ liquid from the submerged island might be channeled elsewhere, or might stop flowing from that particular convection cell. The submerged cell becomes "extinct." This could explain why there is a decrease in the number of convection cell with time, our hypothesis is that some cells get covered by the viscous liquid and become extinct. This would decrease the population of active convection cells with increasing time (as in Fig. 2) or with increasing silica layer thickness (as in Fig. 10), where there are 16–20 cells/mm^2 after 2 h of oxidation, but only 3–4 cells/mm^2 after 6 h of oxidation.

IV. Discussion

The density (no.cells/mm^2) of convection cells for the ZS composite oxidized at 1550°C rapidly increases at the first stage of the oxidation but then decreases slowly with increasing time.

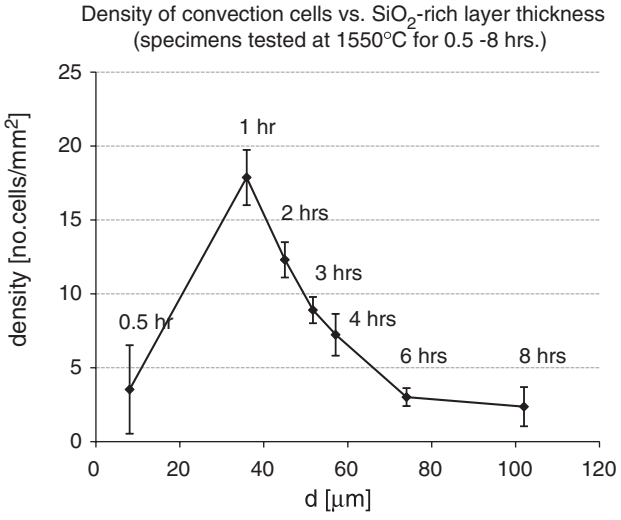

Fig. 10. The number of cells per square mm versus measured thickness of the SiO_2-rich surface layer formed on the ZrB_2–15 vol% SiC composite oxidized from 0.5 to 8 h at 1550°C.

If the density of cells for the ZS composite at 1550°C are compared with the thickness of the SiO_2-rich surface layer the same trend is seen (Fig. 10). This indicates that the convection cells are transient, i.e. perhaps they form and transport BSZ liquid to the surface but then with time the increasing amount of flowing viscous SiO_2-rich liquid submerges them and they become extinct. The "submerged" ZrO_2 islands shown in the cross-section of the ZS-6 and ZS-8 specimens in Fig. 9 support this hypothesis. Perhaps the viscous SiO_2-rich layer is then thick enough to suppress the formation of new convection cells. These result suggest that the convection cell mechanisms is dominant in the early stage of the oxidation of these materials, supplying the SiO_2 to the surface, then when the surface layer becomes mainly viscous SiO_2 the replenishment of the SiO_2 by the formation of convection cells stops and they go "extinct."

V. Summary

The density (no.cells/mm^2) of convection cells for the ZrB_2–SiC composite oxidized at 1550°C increased rapidly from 0.5 to 1 h of exposure time. From 1 to 8 h exposure time the density slowly decreases. The results indicate that the convection cells are transient, they form and transport BSZ liquid to the surface but with increasing exposure time the increasing amount of flowing viscous SiO_2-rich liquid submerges them and they become extinct.

Increased temperature of the ZrB_2–SiC testing (from 1500° to 1600°C) led to increased number of convection cells. This is likely because of more ZrO_2 can precipitate from the BSZ liquid due to increased evaporation rate of B_2O_3 at higher temperatures, which speeds up the formation of the convection cells.

Acknowledgment

We thank Drs. Alida Bellosi and Frederick Monteverde for providing the ZrB_2–SiC composite material used for this study.

References

[1]W. G. Fahrenholtz, "The ZrB_2 Volatility Diagram," *J. Am. Ceram. Soc.*, **88** [12] 3509–12 (2005).
[2]W. G. Fahrenholtz, "Thermodynamics of ZrB_2–SiC Oxidation: The Formation of a SiC-Depleted Region," *J. Am. Ceram. Soc.*, **90** [1] 142–8 (2007).
[3]F. Monteverde, "The Thermal Stability in Air of Hot Pressed Diboride Matrix Composites for Uses at Ultra-High Temperatures," *Corrosion Science.*, **47**, 2020–33 (2005).
[4]M. M. Opeka, I. G. Talmy, and J. A. Zaykoski, "Oxidation-Based Materials Selection for 2000°C+Hypersonic Aerosurface: Theoretical Considerations and Historical Experience," *J. Mater. Sci.*, **39**, 5887–904 (2004).
[5]S. N. Karlsdottir, J. W. Halloran, and C. E. Henderson, "Convection Patterns in Liquid Oxide Films on ZrB_2–SiC Composites Oxidized at a High Temperature," *J. Am. Ceram. Soc.*, **90** [9] 2863–7 (2007).
[6]S. N. Karlsdottir, J. W. Halloran, and A. N. Grundy, "Zirconia Transport by Liquid Convection During Oxidation of Zirconium Diboride–Silicon Carbide Composite," *J. Am. Ceram. Soc.*, **91** [1] 272–7 (2008).
[7]S. N. Karlsdottir and J. W. Halloran, "Formation of Oxide Films on ZrB_2–SiC Composites during Oxidation: Relation of Subscale Recession to Liquid Oxide Flow," *J. Am. Ceram. Soc.*, **91** [11] 3652–8 (2008).
[8]S. N. Karlsdottir, J. W. Halloran, F. Monteverde, and A. Bellosi, "Oxidation of ZrB_2–SiC: Comparison of Furnace Heated Coupons and Self-Heated Ribbon Specimens"; *Proceedings of the 31st International Conference on Ceramics and Composites*, Daytona Beach, FL, January 21–26, 2007.
[9]A. Wackernagel, C. Massone, G. Hoefler, E. Steinbauer, H. Kerl, and P. Wolf, "Plasmacytoid Dendritic Cells are absent in Skin Lesions of Polymorphic Light Eruption," *Photodermatol. Photoimmunol. Photomed.*, **23**, 24–8 (2007).
[10]H. Daims and M. Wagner, "Quantification of Uncultured Microorganisms by Fluorescence Microscopy and Digital Image Analysis," *Appl. Microbiol. Biotechnol.*, **75**, 237–48 (2007).
[11]D. B. Epassaka, S. Ohshio, and H. Saitoh, "Morphological Instability of ZrO_2 Crystallites formed by CVD Technique Operated under Atmospheric Pressure," *J. Mater. Sci.*, **38**, 3239–44 (2003).
[12]Z. Bian, H. Kato, C. L. Qin, W. Zhang, and A. Inoue, "Cu–Hf–Ti–Ag–Ta Bulk Metallic Glass Composites and Their Properties," *Acta Mater.*, **53**, 2037–48 (2005).
[13]W. Vogel, "Crystallization as a Defect in Glass"; pp. 289–90 in Chapter 10.3 *Glass Chemistry*, 2nd edition, Springer-Verlag, Berlin, Germany, 1994.
[14]R. J. Kirkpatrick, "Crystal Growth from the Melt: A Review," *American Mineralogist*, **60**, 798–614 (1975). □